Spatial Aliasing Artifacts Produced by Linear Loudspeaker Arrays used for Wave Field Synthesis

Sascha Spors

Deutsche Telekom Laboratories

Ernst-Reuter-Platz 7, 10587 Berlin, Germany

Sascha.Spors@telekom.de

Abstract—**Spatial sound reproduction systems with a large number of loudspeakers are increasingly being used. Wave field synthesis is a reproduction system using a large number of densely placed loudspeakers (loudspeaker array). This implies a spatial sampling process that may lead to aliasing artifacts. This paper derives the spatial aliasing artifacts of linear loudspeaker arrays used for wave field synthesis and an anti-aliasing condition.**

I. INTRODUCTION

The goal of sound reproduction is to create the perfect acoustic illusion. Various reproduction systems with an increasing number of loudspeakers emerged over the past decades in order to achieve this goal. One of the proposed methods, Wave field synthesis (WFS), aims at reproducing the sound of complex acoustic scenes as natural as possible using densely placed loudspeakers. In theory, WFS creates a physically correct reproduction of virtual wave fields by a continuous distribution of secondary sources placed around the listening area. In practical implementations this distribution will be realized by a limited number of loudspeakers placed at discrete positions. This implies a spatial sampling process that may lead to spatial aliasing artifacts. Typical implementations of WFS systems use (piecewise) linear loudspeaker arrays. An anti-aliasing condition for linear loudspeaker arrays was already derived in [1], [2]. However, no detailed analysis of the aliasing artifacts has been performed. This paper analyzes the spatial aliasing artifacts of linear loudspeaker arrays used for WFS based reproduction and derives an anti-aliasing condition.

This paper is organized as follows: The next section briefly introduces the concept of WFS, followed by a mathematical analysis of the aliasing artifacts produced by infinite and finite length loudspeaker arrays. An application example illustrates the derived results.

II. WAVE FIELD SYNTHESIS

The theory of WFS has been initially developed at the Technical University of Delft [3] and has been developed further by an active research community over the past two decades. Its mathematical foundation for three-dimensional arbitrary shaped volumes is given by the Kirchhoff-Helmholtz integral [1], [3]. Typical implementations of WFS systems are restricted to the reproduction in a plane only using (piecewise) linear loudspeaker arrays. The theoretical basis of WFS for this specialized geometry is
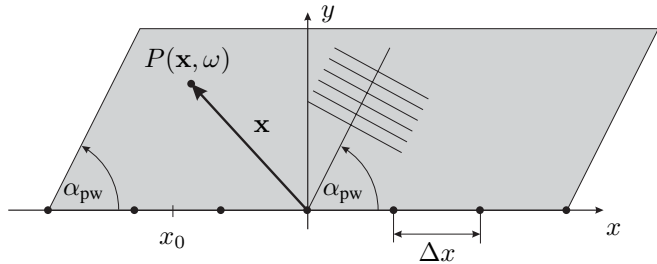

Fig. 1. Geometry used to derive the sampling artifacts for linear loudspeaker arrays. The ● denote the sampling positions of the driving function $D_S(x, \omega)$ and the gray plane the reproduction area for a plane wave with incidence angle α_{pw} using a finite length array.

given by the two-dimensional Rayleigh I integral [1], [3]. The Rayleigh I integral states that a linear distribution of monopole line sources (secondary sources) is capable of reproducing a desired wave field (virtual source) in one of the half planes defined by the linear distribution. The wave field in the other half plane is a mirrored version of the desired wave field, due to the use of monopoles as secondary sources. Without loss of generality the geometry depicted in Fig. 1 is assumed: A linear secondary source distribution which is located on the x-axis ($y = 0$) of a Cartesian coordinate system. The reproduced wave field is given by specializing the two-dimensional Rayleigh I integral to this geometry as follows

$$P(\mathbf{x}, \omega) = \int_{-\infty}^{\infty} \underbrace{2j\omega\rho_0 V_y(\mathbf{x}_0, \omega)}_{D(\mathbf{x}_0, \omega)} \cdot \underbrace{\frac{j}{4} H_0^{(2)}(k\,|\mathbf{x} - \mathbf{x}_0|)}_{G_{2\mathrm{D}}(\mathbf{x} - \mathbf{x}_0, \omega)} \, dx_0 \,,$$

(1)

where ρ_0 denotes the static density of air, $k = \omega/c$ the acoustic wave number, $V_y(\mathbf{x}_0, \omega)$ the particle velocity of the virtual source $S(\mathbf{x}, \omega)$ in direction of the positive y-axis and $H_0^{(2)}(\cdot)$ the zeroth-order Hankel function of second kind. The vector $\mathbf{x}_0$ is defined as $\mathbf{x}_0 = [\ x_0\quad 0\ ]^T$ for the considered geometry. The terms involving the wave field produced by the secondary sources are abbreviated by $G(\mathbf{x} - \mathbf{x}_0, \omega)$ and those involving their strength (driving function) by $D(\mathbf{x}_0, \omega)$. The secondary sources for the 2D case $G_{2\mathrm{D}}$, as given by Eq. (1), can be interpreted as line sources intersecting the listening area at the position $\mathbf{x}_0$ [1].

Practical implementations of WFS systems use closed loudspeakers. These approximately have the characteristics of acoustic point sources. This mismatch in source types may produce various artifacts in the reproduced wave field that only can be corrected to some extend [1], [4]. In the follow-

ing, the effects of sampling are derived for the artifact free case with line sources as secondary sources. However, it is shown later that the obtained results also hold for secondary point sources.

As for time domain sampling, a frequency domain formulation of the signals involved is useful in order to obtain the sampling artifacts. Equation (1) comprises a convolution along the x-axis. Applying a two-dimensional spatial Fourier transformation [5] yields the pressure field in the spatio-temporal frequency domain as

$$\tilde{P}(\mathbf{k}, \omega) = \tilde{D}(k_x, \omega) \, \tilde{G}(\mathbf{k}, \omega) \,, \tag{2}$$

where the respective variables in the spatial frequency domain are labeled by a tilde. The vector $\mathbf{k} = \begin{bmatrix} k_x & k_y \end{bmatrix}^T$ denotes the spatial frequency vector (wave vector), where for acoustic wave fields $|\mathbf{k}| = \omega/c$.

III. SAMPLING ARTIFACTS PRODUCED BY LINEAR LOUDSPEAKER ARRAYS

The driving function $D(x, \omega)$ is sampled at equidistant positions, in order to model the effect of a spatially discrete secondary source distribution. The process of sampling can be described mathematically by multiplying the continuous driving function with a series of Dirac functions

$$D_S(x, \omega) = D(x, \omega) \cdot \frac{1}{\Delta x} \sum_{\mu=-\infty}^{\infty} \delta(x - \Delta x \mu) \,, \tag{3}$$

where $D_S(x, \omega)$ denotes the sampled driving function and Δx the distance (sampling period) between the sampling positions. These positions are indicated in Fig. 1 by the dots •. The result of sampling is a series of weighted Dirac pulses at the sampling positions. The spatio-temporal spectrum of the sampled driving function can be calculated by applying a spatial Fourier transformation to Eq. (3) with respect to the x-coordinate

$$\tilde{D}_S(k_x, \omega) = 2\pi \sum_{\eta=-\infty}^{\infty} \tilde{D}_{\mathsf{C}}(k_x - \frac{2\pi}{\Delta x}\eta, \omega) \,. \tag{4}$$

As for time domain sampling, spatial sampling results in a repetition of the spectrum of the continuous driving function $\tilde{D}(k_x, \omega)$ on the spatial frequency k_x-axis. Introducing $\tilde{D}_S(k_x, \omega)$ into Eq. (2) yields the spectrum of the wave field $\tilde{P}_S(\mathbf{k}, \omega)$ produced by a sampled secondary source distribution

$$\tilde{P}_S(\mathbf{k}, \omega) = 2\pi \sum_{\eta=-\infty}^{\infty} \tilde{D}(k_x - \frac{2\pi}{\Delta x}\eta, \omega) \, \tilde{G}(\mathbf{k}, \omega) \,. \tag{5}$$

The reproduced wave field for a spatially sampled secondary source distribution is given by the sampled driving function $\tilde{D}_S(k_x, \omega)$ weighted by the spectrum $\tilde{G}(\mathbf{k}, \omega)$ of the secondary sources. Hence, spatial sampling of the secondary source distribution can be understood as a sampling and interpolation process. The interpolator is given by the characteristics of the secondary sources.

In order to derive the effects of spatial sampling and a sampling theorem, the spatio-temporal spectrums of the secondary sources $\tilde{G}(\mathbf{k}, \omega)$ and the driving function $\tilde{D}(k_x, \omega)$ have to be considered. The spatial Fourier transformation of a secondary line source can be calculated by way of its Hankel transformation. It is given as

$$\tilde{G}_{\mathrm{2D}}(\mathbf{k}, \omega) = -\frac{1}{4(k_x^2 + k_y^2 - (\frac{\omega}{c})^2)} +$$
$$+ \frac{j}{4\sqrt{k_x^2 + k_y^2}} \delta(\sqrt{k_x^2 + k_y^2} - \frac{\omega}{c}) \,. \tag{6}$$

The spectrum of the driving function $\tilde{D}(k_x, \omega)$ depends from the wave field of the virtual source $S(\mathbf{x}, \omega)$. It is sufficient to consider a plane wave as wave field for the virtual source, since arbitrary wave fields can be decomposed into plane waves [5]. The following section derives the sampling artifacts for the reproduction of plane waves.

A. Sampling Artifacts for the Reproduction of Plane Waves

The wave field of a monochromatic plane wave with incidence angle α_{pw} is given as [5]

$$S_{\mathrm{pw}}(\mathbf{x}, \omega) = e^{-j\frac{\omega}{c}(x \cos \alpha_{\mathrm{pw}} + y \sin \alpha_{\mathrm{pw}})} \,, \tag{7}$$

where α_{pw} denotes the incidence angle of the plane wave (see Fig. 1). The driving signal for the reproduction of a plane wave is given according to Eq. (1) as

$$D_{\mathrm{pw}}(x, \omega) = -2j \frac{\omega}{c} \sin(\alpha_{\mathrm{pw}}) \, e^{-j\frac{\omega}{c} x \cos \alpha_{\mathrm{pw}}} \,. \tag{8}$$

For the upper half plane ($y > 0$), the secondary source distribution is only capable of reproducing plane waves traveling into the positive y-direction [1], [3]. Thus, it is reasonable to limit the incidence angle of the virtual plane waves to $0 \leq \alpha_{\mathrm{pw}} < \pi$ in the following. Calculating the spectrum $\tilde{D}_{\mathrm{pw}}(k_x, \omega)$ of the driving signal and introducing it together with the spectrum of the secondary sources (6) into Eq. (5) derives the reproduced wave field $\tilde{P}_{S,\mathrm{pw}}(\mathbf{k}, \omega)$ as

$$\tilde{P}_{S,\mathrm{pw}}(\mathbf{k}, \omega) = \pi \frac{\omega}{c} \sin \alpha_{\mathrm{pw}} \sum_{\eta=-\infty}^{\infty} \delta(k_x - \frac{2\pi}{\Delta x}\eta - \frac{\omega}{c} \cos \alpha_{\mathrm{pw}})$$
$$\times \left(\frac{1}{k} \delta(\sqrt{k_x^2 + k_y^2} - \frac{\omega}{c}) + j \frac{1}{k_x^2 + k_y^2 - (\frac{\omega}{c})^2} \right) \,. \tag{9}$$

The reproduced spectrum consists of a real and an imaginary part. The imaginary part can be identified as being produced by the near-field of the secondary sources. This part is neglected first for the derivation of the sampling artifacts. For a fixed temporal frequency ω, the first Delta function in the real part of Eq. (9) can be interpreted as a series of Dirac lines perpendicular to the k_y-axis at the positions $k_x = \frac{2\pi}{\Delta x}\eta + \frac{\omega}{c} \cos \alpha_{\mathrm{pw}}$. The second Delta function can be interpreted as a circular Dirac pulse with the radius $\frac{\omega}{c}$. Figure 2 illustrates the real part of $\tilde{P}_{S,\mathrm{pw}}$ in the spatial k_x-k_y-frequency plane. Due to the sifting property of Dirac functions, the result of the multiplication of the two Dirac functions is given by their intersections in the spatial frequency plane. The result for $\eta = 0$ comprises the desired plane wave. The other terms in the sum for $\eta \neq 0$ are potential aliasing contributions.
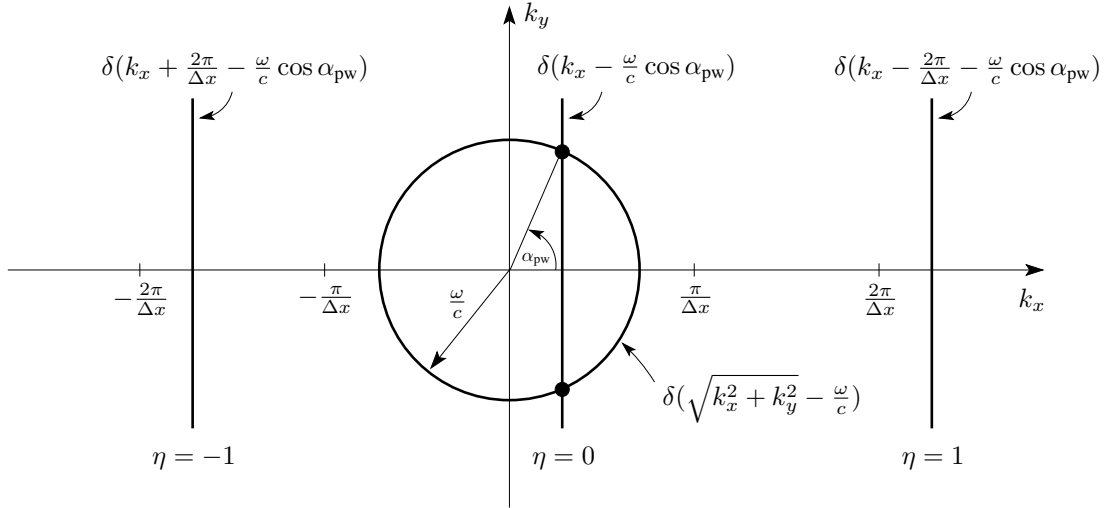
Fig. 2. Illustration of the real part of the spectrum $\tilde{P}_S$ reproduced by a discrete secondary monopole source distribution for the reproduction of a plane wave with incidence angle α_{pw}. The resulting spectrum is given by the intersection of the two Dirac functions at the positions indicated by the dots ●.

For the situation shown in Fig. 2, the result are two Dirac's at the positions indicated by the dots ●. In this particular example, these two Dirac's represent the desired wave field of a plane wave traveling into the positive y-direction for the upper half plane ($y > 0$) and into the negative y-direction for the lower half plane ($y < 0$). This symmetry results from the reproduction using only secondary monopole sources.

For an increasing distance Δx between the secondary sources there may also be additional contributions besides the desired plane wave in the reproduced wave field. In this case, the repetitions of the Dirac lines in the real part of Eq. (9) for $\eta \neq 0$ move towards the circular Delta function. If these repetitions overlap with the circular Delta function additional plane wave contributions result. These contributions constitute spatial aliasing due to spatial sampling of the secondary source distribution. They are avoided if the frequency of the reproduced plane wave is limited. An anti-aliasing condition for the driving function can be derived from Fig. 2 and Eq. (9) as

$$\omega \leq \frac{2\pi\, c}{\Delta x\, (1 + |\cos \alpha_{\text{pw}}|)}\,. \tag{10}$$

Thus, a reduction of the temporal frequency of the reproduced monochromatic plane wave avoids spatial aliasing present in the reproduced wave field. For an arbitrary wave field condition (10) has to be fulfilled for the minimum and maximum incidence angle and the highest frequency of its plane wave contributions. Please note that the condition (10) differs from the one derived in [1] since the propagation characteristics of the secondary sources are included.

If the anti-aliasing condition (10) is not fulfilled, aliasing artifacts will be present in the reproduced wave field. According to Fig. 2 and Eq. (9) these artifacts are a superposition of plane waves (for $\eta \neq 0$) with different incidence angles than the desired plane wave. However, only those spectral repetitions of the Dirac lines result in spatial aliasing contributions where the circular Dirac pulse and the Dirac lines in Fig. 2 intersect. Hence, only a subset η_{al} of all possible spectral repetitions η will be present in the reproduced wave field for a particular incidence angle and frequency of the desired plane wave. This subset includes all $\eta_{\text{al}} \in \mathbb{Z}\backslash 0$ for which the following condition holds

$$\left| \frac{2\pi}{\Delta x}\eta_{\text{al}} + \frac{\omega}{c}\cos\alpha_{\text{pw}} \right| \leq \frac{\omega}{c}\,. \tag{11}$$

Using this subset, the incidence angles $\alpha_{\eta_{\text{al}}}$ of the plane waves representing aliasing can be derived from Eq. (9) as

$$\cos\alpha_{\text{pw},\eta_{\text{al}}} = \frac{\frac{2\pi}{\Delta x}\eta_{\text{al}} + \frac{\omega}{c}\cos\alpha_{\text{pw}}}{\frac{\omega}{c}}\,. \tag{12}$$

Up to now, only the real part of the reproduced spectrum was considered. The poles of the imaginary part are also located on the circle shown in Fig. 2. Applying the sifting property of the Delta function, the spectrum of these contributions is given by evaluation the imaginary part at $k_x = \frac{2\pi}{\Delta x}\eta + \frac{\omega}{c}\cos\alpha_{\text{pw}}$. The result is not bandlimited in the k_y but in the k_x direction. Hence, the anti-aliasing condition (10) applies also to the imaginary part. The aliasing contributions of the imaginary part have the form of evanescent plane waves.

B. Truncated Loudspeaker Arrays

Up to now, the linear secondary source distribution was assumed to be of infinite length. However, practical implementations of linear loudspeaker arrays will always be of finite length. It is shown in the following that this truncation has consequences on the aliasing artifacts derived in the previous section.

The truncation of the infinite secondary source distribution can be modeled by multiplying the loudspeaker driving function $D(x,\omega)$ with a rectangular window function. The multiplication with this window function leads to a convolution with a sinc function in the spatial frequency domain. The effects of truncation for linear arrays have been discussed in detail by [1], [3]. For simplicity these effects are approximated only in the following.

For the reproduction of plane waves, the effect of truncation can be approximated quite well by simple geometric means, as illustrated by the gray area in Fig. 1. This approximation states that a plane wave will be reproduced only in a

tilted rectangular area in front of the array, whose width is equivalent to the aperture of the array and length is infinite. The area is tilted by the incidence angle α_{pw} of the plane wave to be reproduced. Outside of this area the energy of the reproduced wave field will be quite low. Inside of this area the reproduced wave field will approximately match the virtual source wave field when neglecting sampling. Some aperture artifacts will be present [1], [3].

As a consequence to this limited reproduction area, the aliasing effects discussed above depend on the listener position. This is due to the fact, that not all plane waves can be reproduced at all listener positions. Those plane waves who are relevant at a given listener position can be found easily by the geometric approximation discussed above (see also Fig. 1).

A special case is represented by a plane wave with an incidence angle of $\alpha_{\mathrm{pw}} = 90^{\mathrm{o}}$ and listener positions far away from the array: no aliasing artifacts are present here. The aliasing frequency is infinite for this case.

C. Secondary Point Sources

Typical implementations of two-dimensional WFS systems use point sources (loudspeakers) instead of line sources as secondary sources. The wave field produced by a point source is given by the 3D free-field Green's function $G_{\mathrm{3D}}(\mathbf{x} - \mathbf{x}_0, \omega)$ [5]. The spatial Fourier transformation of G_{3D} is given as

$$\tilde{G}_{\mathrm{3D}}(\mathbf{k}, \omega) = \frac{1}{4\pi} \frac{1}{\sqrt{k_x^2 + k_y^2 - (\frac{\omega}{c})^2}} . \qquad (13)$$

The poles of the spatial Fourier transformation $\tilde{G}_{\mathrm{3D}}(\mathbf{k}, \omega)$ are again located on a circle with radius $\frac{\omega}{c}$ in the k_x-k_y-domain. Due to the same reasons as for the imaginary part of secondary line sources, the sampling theory presented so far can also be applied to secondary point sources.

D. Application Example

In the following example the reproduction of a monochromatic plane wave with an incidence angle of $\alpha_{\mathrm{pw}} = 90^{\mathrm{o}}$ and a frequency of $f_0 = 10$ kHz using a linear discrete distribution of secondary line sources is considered. The sampling distance between the secondary sources is chosen to $\Delta x = 0.15$m. Figure 3 illustrates the incidence angles of the reproduced plane waves in a polar diagram for an array with infinite length. Each line represents a plane wave traveling into the depicted direction. The dashed line represents the desired plane wave, the solid lines the aliasing contributions. Besides the desired plane wave, eight plane waves constituting aliasing are reproduced in this particular example.

The gray wedge shown in Fig. 3 illustrates the effect of truncation for an array with a total length of $l = 2$ m and a listener position in the center of the array ($x_l = 0$ m) at a distance of $y_l = 1$ m. Only plane wave contributions within the angles depicted by the gray wedge are reproduced.
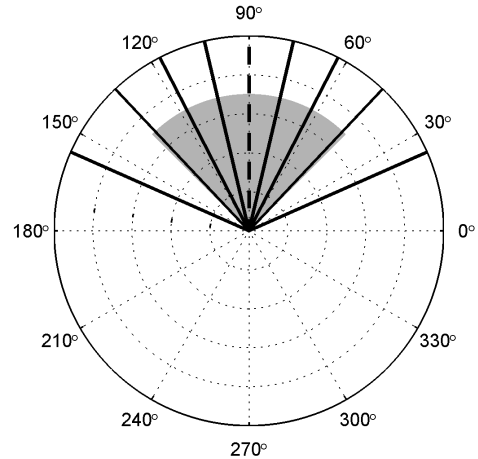

Fig. 3. Incidence angle of the desired plane wave α_{pw} (dashed line) and its aliasing contributions $\alpha_{\mathrm{pw},\eta_{\mathrm{al}}}$ (solid lines). The gray wedge illustrates the effect of truncation for one particular listener position.

IV. CONCLUSION

The presented theory of spatial sampling for linear loudspeaker arrays revealed that for the reproduction of monochromatic plane waves, spatial aliasing can be interpreted as plane waves itself. Due to the aperture effects of finite length linear arrays these aliasing artifacts depend from the listener position.

For reproduction purposes spatial aliasing does not play a dominant role since the human auditory system doesn't seem to be too sensible for spatial aliasing [1], [3]. A loudspeaker distance of $\Delta x = 10 \ldots 30$ cm has proven to be suitable in practice for reproduction only purposes. However, spatial aliasing limits the application of techniques like active listening room compensation [6], active noise control (ANC) and acoustic echo cancelation (AEC).

Since typical listening rooms exhibit a rectangular shape, rectangular arrays are frequently used to build WFS systems. Rectangular arrays can be regarded as a superposition of truncated linear arrays. Hence, the sampling theory introduced in this paper can be applied with minor changes to rectangular geometries.

REFERENCES

[1] E.W. Start, *Direct Sound Enhancement by Wave Field Synthesis*, Ph.D. thesis, Delft University of Technology, 1997.

[2] D. Leckschat and M. Baumgartner, "Wellenfeldsynthese: Untersuchungen zu Alias-Artefakten im Ortsfrequenzbereich und Realisierung eines praxistauglichen WFS-Systems," in *31. Deutsche Jahrestagung für Akustik*, Munic, Germany, 2005.

[3] A.J. Berkhout, D. de Vries, and P. Vogel, "Acoustic control by wave field synthesis," *Journal of the Acoustic Society of America*, vol. 93, no. 5, pp. 2764–2778, May 1993.

[4] S. Spors, M. Renk, and R. Rabenstein, "Limiting effects of active room compensation using wave field synthesis," in *118th AES Convention*, Barcelona, Spain, May 2005, Audio Engineering Society (AES).

[5] E.G. Williams, *Fourier Acoustics: Sound Radiation and Nearfield Acoustical Holography*, Academic Press, 1999.

[6] S. Spors, H. Buchner, and R. Rabenstein, "A novel approach to active listening room compensation for wave field synthesis using wave-domain adaptive filtering," in *IEEE International Conference on Acoustics, Speech, and Signal Processing (ICASSP)*, 2004.